SUBMITTED TO ApJ
Preprint typeset using LaTeX style emulateapj v. 10/09/06

MHD SIMULATIONS OF PENUMBRA FINE STRUCTURE

T. HEINEMANN[1]
Department of Applied Mathematics and Theoretical Physics, Centre for Mathematical Sciences, Wilberforce Road, Cambridge CB3 0WA, United Kingdom

Å. NORDLUND
Niels Bohr Institute, University of Copenhagen, Juliane Maries Vej 30, 2100 Copenhagen, Denmark

G.B SCHARMER
Institute for Solar Physics, Royal Swedish Academy of Sciences, AlbaNova University Center, SE-106 91 Stockholm, Sweden

AND

H.C. SPRUIT
Max Planck Institute for Astrophysics, Box 1317, 85741 Garching, Germany
Submitted to ApJ

ABSTRACT

We present results of numerical 3D MHD simulations with radiative energy transfer of fine structure in a small sunspot of about 4 Mm width. The simulations show the development of filamentary structures and flow patterns that are, except for the lengths of the filaments, very similar to those observed. The filamentary structures consist of gaps with reduced field strength relative to their surroundings. Calculated synthetic images show dark cores like those seen in the observations; the dark cores are the result of a locally elevated $\tau = 1$ surface. The magnetic field in these cores is weaker and more horizontal than for adjacent brighter structures, and the cores support a systematic outflow. Movies show migration of the dark-cored structures towards the umbra, and fragments of magnetic flux that are carried away from the spot by a large scale 'moat flow'. We conclude that the simulations are in qualitative agreement with observed penumbra filamentary structures, Evershed flows and moving magnetic features.

Subject headings: sunspots – magnetic field

1. INTRODUCTION

Explaining the magnetic field, Evershed flow, overall fine structure of sunspot penumbrae and the observed high heat flux (~75% of that of the quiet sun atmosphere), constitute some of the most longstanding problems in solar physics. Despite nearly a century of detailed studies, no consensus has been reached as regards the origin, or even morphology, of this fine structure. A major obstacle to progress is our inability to adequately resolve sunspot fine structure when observations are carried out with spectrographs or spectropolarimeters. The discovery of dark-cored penumbra filaments (Scharmer et al. 2002) suggests that the basic elements of penumbral structure are now observable with imaging instrumentation.

Ambiguities associated with interpretations of existing observational data have given rise to a diversity of models and explanations for flows and fine structure in penumbrae (e.g., Meyer & Schmidt 1968, Solanki & Montavon 1993, Schlichenmaier et al. 1998a,b, Thomas et al. 2002, Spruit and Scharmer 2006). In contrast to what is the case for granulation (e.g., Stein and Nordlund 1998), faculae (Carlsson et al. 2004, Keller et al. 2004, Steiner 2005) and umbral dots (Schüssler & Vögler 2006), realistic numerical simulations of entire sunspots have not yet been feasible. This is partly due to difficulties of thermally relaxing such a deep structure and maintaining its stability, but mostly due to the huge range of scales associated with a fully developed sunspot.

[1] Previously at: NORDITA, AlbaNova University Center, 10691 Stockholm, Sweden

1.1. *The gappy penumbra*

Spruit and Scharmer (2006 – hereinafter SS06a) have pointed to a similarity between penumbral filaments and light bridges, the bright lanes often seen crossing an umbra. Both have a dark core: a narrow dark lane along their mid-line. In SS06a it was argued that this is not just an observational congruence, but that the similarity actually indicates a common origin for these structures: gaps in the magnetic field, closing near the visible surface, and heated by convection in the gap. In Scharmer and Spruit (2006 – hereinafter SS06b) magnetostatic models for such structures were presented. Their properties, distinctly different in the inner and outer penumbra, are consistent with a number of observations, such as the differences in strength and inclination of the magnetic field between dark and bright penumbral structure.

Radiative MHD simulations of light bridges by one of the authors (ÅN, unpublished) and Heinemann (2006) show how the dark cores over the center of the light bridges are formed. They are found to be a consequence of hydrostatic pressure and radiative energy balance around the 'cusp' of the magnetic field, at the height in the atmosphere where field lines from both sides close over the gap. A second observational clue is given by umbral dots, which are often seen to evolve from the 'heads' of penumbral filaments propagating into the umbra. As proposed by Parker (1979), seen in numerical simulations by Nordlund & Stein (1990), and recently confirmed through high resolution numerical simulations by Schüssler and Vögler (2006), umbral dots are the surface manifestation of nearly field-free gaps below the umbral photosphere. This theoretical evidence is strengthened observationally by

the short dark cores seen to cross peripheral umbral dots (Scharmer et al. 2002).

High-resolution images of complex sunspot groups (e.g., Fig. 1 of Rouppe van der Voort et al. 2004) show penumbra structures associated with both small and large, symmetric and irregular sunspots, and even penumbrae without visible umbrae. This suggests that there is no need to model entire sunspots to explain penumbra fine structure. This, and the rapid formation of penumbrae with well developed Evershed flows (Leka & Skumanich 1998, Yang et al. 2003), also suggest that details of the deep structure of the magnetic field may not be crucial for these structures. In this paper, we describe first results from realistic simulations of penumbral fine structure. The model used for these simulations is a rectangular section of the solar atmosphere containing a part of a sunspot with umbra and penumbra, embedded in an essentially field-free atmosphere. The simulations show the development of short filamentary structures, associated with the formation of gaps with strongly reduced field strength. They resemble observed penumbral filaments as seen in the inner penumbra: like these, they have a characteristic head-and tail structure with a dark core running along the tail, and are seen to propagate inward.

2. MHD SIMULATIONS

The simulations were carried out using the PENCIL code[2], modified to handle energy transfer by radiation in a grey atmosphere (Heinemann 2006, Heinemann et al. 2006). We used a rectangular computational box 12448×6212 km in the horizontal (x and y) directions, extending over a depth (z) range of 3094 km and with a grid separation of 24.36 km in both horizontal and vertical directions ($512 \times 256 \times 128$ grid points). The quiet sun photosphere is located approximately 700 km below the upper boundary. In the horizontal directions, periodic boundary conditions are used. Both the upper and lower boundaries are closed in the sense of not allowing vertical flows. The vertical magnetic field component is kept fixed at the lower boundary. To avoid inconsistencies with that boundary condition, the horizontal velocity is set to zero at the lower boundary. The magnetic field is free to evolve at the upper boundary.

The initial magnetic field of the simulations is a potential (current-free) magnetic field, initially depending only on x and z, separated by a current sheet from the surrounding convection zone. This initial magnetic field is defined by two free parameters, the total vertical flux and the ratio of gas pressure to magnetic pressure, β, along the current sheet. For all calculations made, β was assumed to be independent of depth. The corresponding potential field, given by magnetostatic equilibrium with a gas pressure obtained from a convection simulation and the chosen value of β, was calculated with the method described in SS06b. Since the subsequent magnetic field evolution is driven by the internal dynamics of the model, the choice of the total vertical flux and β primarily constrains the width and field strength of the flux bundle close to the lower boundary.

We made several simulations with different values for the total vertical flux and β. All simulations showed the formation of dark-cored filamentary structures, but with variations in their morphology, number density and life times. Here we discuss only the results of one of these simulations, obtained with an average vertical field strength of 1 kG and $\beta = 19$, corresponding to an initial ratio of the gas pressures in the magnetic to non-magnetic components of $\beta/(\beta + 1) = 0.95$. The initial magnetic field configuration is shown in Fig. 1 (upper panel).

[2] see http://nordita.dk/software/pencil-code

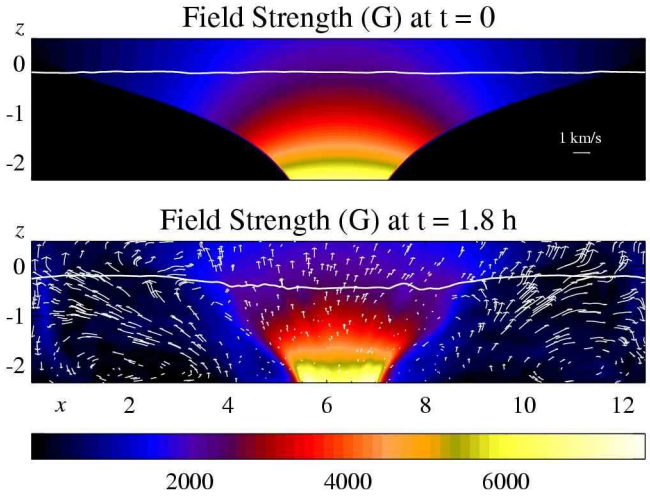

FIG. 1.— Magnetic field strength for the initial state (upper panel) and averaged over the y-axis for the snapshot seen in Fig. 2 (lower panel). Also shown are contours of constant optical depth $\tau = 1$. The lower panel shows the average flow field (arrows).

The temperature, gas pressure, and velocity field were initialized from a field-free convection simulation. The gas pressure in the magnetic atmosphere was then reduced by multiplication of the mass density by $\beta/(\beta + 1)$ and the magnetic field was added to the model. The strong suppression of convection by the magnetic field causes a rapid drop in temperature, leading to a strong reduction in gas pressure above the umbra and hence a partial collapse of the magnetic field configuration. After approximately 30 solar minutes, the gas reached a quasi-equilibrium state. The magnetic field strength and flow field (arrows) after approximately 1.8 solar hours, averaged over the y-direction, are shown in Fig. 1 (lower panel).

We assumed a 6th order hyperdiffusivity of $2 \cdot 10^{-9}$ and a shock diffusivity of 5 (cf. Eqs. (130) and (44) of the PENCIL code documentation – see the footnote), in units where length is measured in megameters and time is measured in kiloseconds. The hyperdiffusivity is adequate to avoid the development of ripples at the grid scale, while leaving larger structures essentially inviscid and non-resistive. The shock diffusivity ensures that shocks – which are ubiquitous in the upper photosphere – are adequately resolved by the difference scheme. Radiative energy transfer was handled using 6 rays along the coordinate axes.

3. RESULTS

3.1. *Dark-cored filamentary structures*

Following the initial dramatic adjustment of the model to the applied magnetic field, convection forms small intrusions in the magnetic atmosphere, propagating towards the umbra. Dark lanes, similar to the dark cores of penumbral filaments (Scharmer et al. 2002), form rapidly. A statistically stable situation is reached, where filaments continuously form and disappear on time scales on the order of 30 min.

Figure 2 shows a snapshot after 1.8 solar hours of the emergent intensity and the field strength for a vertical slice of the model at the location of the dotted line in the intensity im-

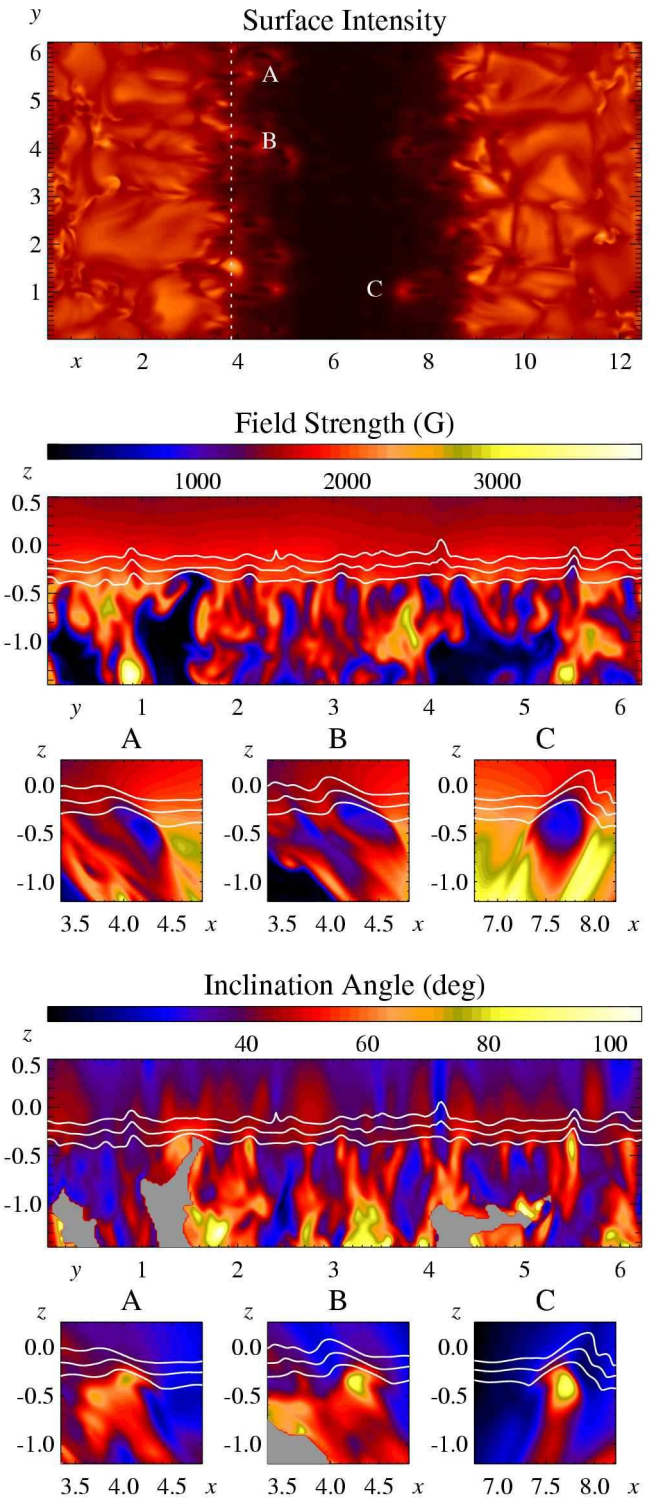

FIG. 2.— Emergent intensity and false-color images of the magnetic field strength and inclination along the dotted line in the intensity image. The six small panels show the field strength and inclination for cuts along three dark-cored filamentary structures (indicated A–C) in the direction perpendicular to the dotted line. The white curves indicate the heights for which (top to bottom) $\tau = 0.01, 0.1, 1$. Tick-marks and axis labels indicate units in Mm.

age. The intensity image shows several short dark-cored filamentary structures protruding into the umbra. The cross-section of the field strength shows several gaps with strongly reduced field strength near the visible surface, while deeper down the magnetic field is strongly fragmented with many and nearly field-free gaps. Also shown in Fig. 2 is the magnetic field strength and inclination of three dark-cored filaments along cuts perpendicular to the dotted line in the intensity image. These cuts show intrusions with strongly reduced field strength that extend over approximately 400 km in depth, and that appear similar to the nearly field-free gaps in the umbral dot simulations of Schüssler and Vögler (2006). These cuts also demonstrate that the gaps are tilted and roughly aligned with the surrounding magnetic field and that the field is nearly horizontal at locations of these filamentary structures near the surface. Shown in Fig. 2 are also contours of constant optical depth for $\tau = 0.01$, 0.1, and 1 (top to bottom). Three of the dark-cored filaments are associated with $\tau = 1$ surfaces that are locally elevated by approximately 100–200 km, implying a strongly localized warping of the visible surface. At heights of only 100–200 km above the $\tau = 1$ layer, the magnetic field is largely homogeneous, with only small horizontal variations in field strength.

In Fig. 3 is shown horizontal variations in the field strength and inclination angle at the height where (locally) $\tau = 1$ for the left-hand side of the umbra-penumbra shown in Fig. 2. This shows several filamentary structures with strongly reduced field strength and nearly horizontal magnetic field at the center of the filaments. Several of these have widths that are only slightly in excess of 100 km, suggesting that they are not adequately resolved with the grid separation used. Figure 3 also shows that the gaps are more numerous, but otherwise similar, 200 km below the visible surface.

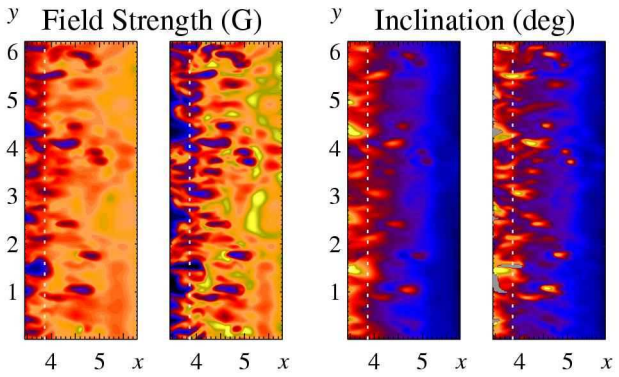

FIG. 3.— False-color images of the field strength and inclination angle at $\tau = 1$ (left) and 200 km below $\tau = 1$ (right) for the left part of the umbra-penumbra shown in Fig. 2. The color look-up tables are the same as shown in Fig. 2

Fig. 4 shows the calculated emergent intensities corresponding to a heliocentric distance of 45°. On the limb-side, at least five round umbral dot-like structures are seen. On the disk-center side, the same dots are fainter, less distinct and partly masked by dark cores. These differences between the limb side and disk center side of penumbrae are in excellent qualitative agreement with observations (Tritschler et al. 2004, Sütterlin et al. 2004, Langhans et al. 2006). The explanation for the enhanced visibility of bright dots on the limb side is essentially the same 'limb brightening' effect seen in faculae: the line of sight is more perpendicular to the $\tau = 1$ surface on the limb side, allowing us to see deeper into the hotter layers of the convecting gas (Spruit 1976, Carlsson et al. 2004, Keller et al. 2004).

Movies of the synthetic intensity images show dark-cored

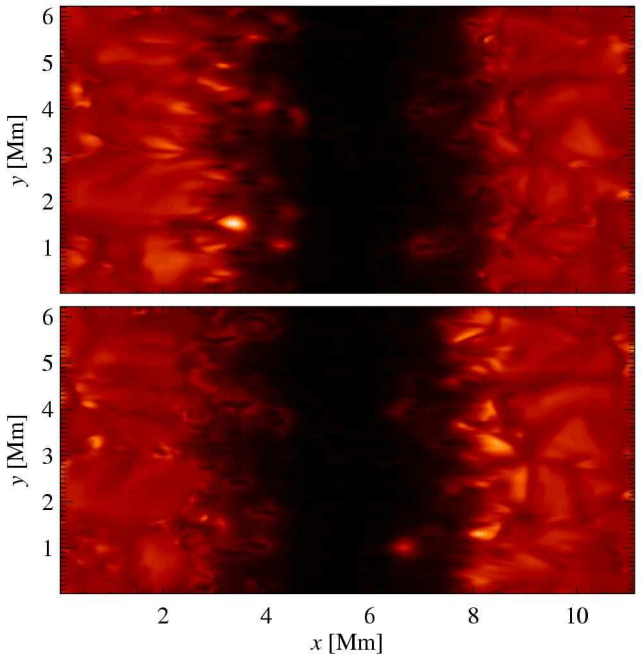

FIG. 4.— Calculated synthetic images corresponding to a heliocentric distance of 45°. In the top image, the limb direction is left, in the bottom image the limb direction is right. To facilitate comparison with the corresponding disk-center image (Fig. 2), the fore-shortening of the image in the horizontal direction has been compensated for.

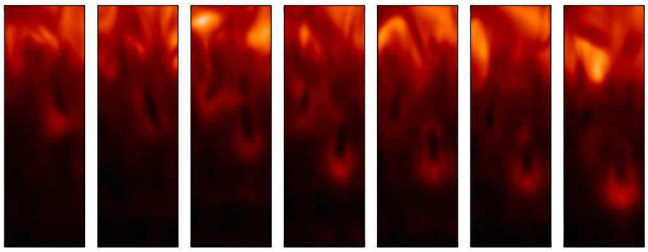

FIG. 5.— Evolution and inward migration of the dark-cored structure labeled 'C' in Fig. 2 during 20 solar minutes. The last snapshot is from the larger field-of-view shown in Figs. 2 and 3.

filamentary structures forming and migrating toward or into the umbra. Several of these structures are significantly darker than observed penumbral filaments, resembling instead the faint dark-cored structures described by Scharmer et al. (2002). Figure 5 shows snapshots taken at 86.7, 90, 93.3, 96.7, 100, 103.3, and 106.7 solar minutes for one such faint dark-cored filament (labeled 'C' in Fig. 2), demonstrating the development of a dark core and the inward migration of the structure. During the time interval of 20 solar minutes shown in this figure, this structure propagates approximately 850 km toward and into the umbra, corresponding to a propagation speed of 0.7 km s^{-1}. This is similar to the inward propagation speeds of approximately 0.5–1 km s^{-1} found by Rimmele and Marino (2006) and the 300 m s^{-1} found by Langhans et al. (2006).

3.2. *Flows associated with dark-cored filaments*

Figure 6 shows horizontal (left panels) and vertical (right panels) maps of flow velocities at $z = -0.23$, -0.35, -0.47, and -0.60 (top to bottom) Mm for two dark-cored filamentary structures shown in Fig. 2. These flow maps show strong upflows in the dot-like brightening and weaker *downflows* outward and to the sides of the strong upflow, clearly demonstrating evidence for overturning convection within the gap. The downflows are not associated with polarity reversals in Fig. 7 and not aligned with the magnetic field. The simulated flows are therefore quite different from (siphon) flows within flux tubes. Above $z = -0.35$, the magnitude of the upflow strongly decreases with height whereas the horizontal outflow peaks at that height. The dark cores are thus associated with flows that have a strong horizontal flow component near the photoshere and that are roughly aligned with the dark core. Similar flows along dark cores were found also in the umbral dot simulations by Schüssler and Vögler (2006). Inspection of movie sequences of the horizontal and vertical flow components at $\tau = 1$ verifies that strong outflows are indeed seen in all gaps. Flows along dark cores were reported by Rimmele and Marino (2006) and Langhans et al. (2006). Although the observed flow channels are much longer than in the simulations, the simulated sunspot appears to develop flows similar to observed Evershed flows. The strong upflows at the innermost footpoint reported by Rimmele and Marino (2006) are also reproduced by our simulations. These authors interpret the observed upflows as evidence in support of uni-directional flows along flux tubes, as seen in the simulations by Schlichenmaier (1998a,b). The simulations made here show similar upflows, but in connection with a more complex flow pattern involving overturning convection.

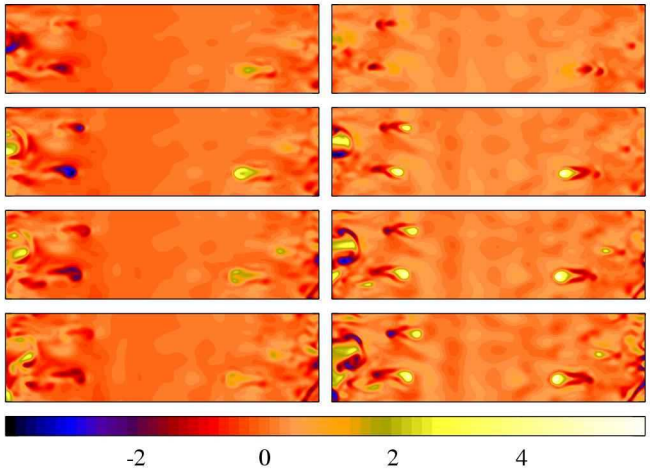

FIG. 6.— Horizontal (left) and vertical velocities at $z = -0.23$, -0.35, -0.47, and -0.60 (top to bottom) for the dark-cored structures on opposite sides of the umbra in the lower part of Fig. 2.

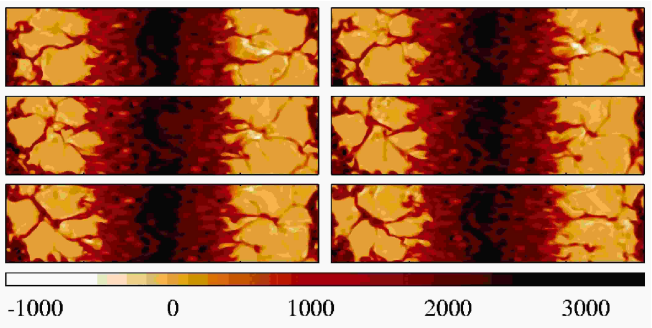

FIG. 7.— Time sequence illustrating the moat flow. The panels (size 12×3 Mm) show the vertical magnetic field component at $\tau = 1$ at time intervals of 200 s. The frames are ordered top-left, top-right, ..., bottom-right.

3.3. *Moat flows*

Figure 1 shows an accumulation of magnetic flux at the boundaries of the computational box and also in the deeper layers below the atmosphere . This accumulation of flux is in part due pumping down of high-β magnetic gas by convection, and in part due to a large-scale circulation pattern, shown by arrows in the lower panel. Movies of the vertical component of the magnetic field at $\tau = 1$ show a continuous shredding of magnetic flux from the sunspot and an outward movement of these structures; a time sequence of such a 'magnetogram' sequence is shown in Fig. 7. We note that some of this shredded flux has a polarity that is opposite to that of the spot. Our simulation therefore appears to produce moving magnetic features and moat flows similar to those seen in magnetogram and continuum movies (e.g, Hagenaar and Shine 2005).

4. DISCUSSION AND CONCLUSIONS

The present simulations, though of restricted scope, already demonstrate that nearly field-free gaps in the penumbra do form, as inferred from the observations by SS06a. The presence of up-flows as well as down-flows within the field-free gaps shows that these gaps are associated with overturning convection, rather than uni-directional (siphon) flows. The structures found in the simulations have several properties in common with observed filaments. They propagate into the umbral magnetic field, and have a dark core overlying the center. The inward facing head of the structure looks similar to tips of filaments, as observed at the boundary between umbra and penumbra. The magnetic field in the simulations shows strong fluctuations of the magnetic field inclination across dark-cored filaments. These variations agree with a number of independent observations (see discussion in SS06a and references therein). The dark-cored structures also are associated with outflows that appear similar to Evershed flows and strong upflows at their innermost footpoints, as observed (e.g, Rimmele and Marino 2006). Synthetic images calculated for a heliocentric distance of 45° show distinct differences between the limb side and disk center side that agree with observations. These are the presence of bright dot-like features on the limb side but not disk center side (Sütterlin et al. 2004, Tritschler et al. 2004, Langhans et al. 2006) and the better visibility of dark cores on the disk center side (Sütterlin et al. 2004, Langhans et al. 2006).

The simulated sunspot develops a large scale moat flow that carries fragments of magnetic flux from the sunspot to the boundary of the computational box. Some of this flux shows up with a polarity opposite to that of the sunspot. These aspects of the simulations are also in qualitative agreement with the observations.

In other respects, the structures appearing in the simulations are not yet fully realistic. The filamentary structures are quite short, and resemble the structure observed near the umbra/penumbra boundary more than the penumbra itself. Also, observations indicate filament lifetimes on the order of 1–2 h, whereas the simulated filaments form and disappear within a typical time span of 30 min.

These differences may be due to the shallow depth and limited horizontal extent of the computational box, which in turn restricts the size of the umbra to a (linear) diameter of approximately 4 Mm. Indeed, observations occasionally show pores with diameters as large as 7 Mm without penumbrae (Bray and Loughhead 1964). An aggravating factor could be the periodic boundary condition of the simulation in the 'radial' direction, which is equivalent to having umbrae of the same polarity next to each other. In observations of neighboring spots of the same polarity, the penumbra is usually suppressed on the side facing the neighboring spot. The lower boundary condition used, which keeps the field fixed there, possibly restricts the horizontal extent of developing structure to something comparable with the depth of the box. This could be tested with changes in the lower magnetic boundary condition or its depth.

Overall, we conclude that the approach to modeling sunspot fine structure by restricting the computational box to a rectangular section of a spot is a viable method to deal with the huge range of scales associated with a mature sunspot.

A number of improvements of these simulations are desirable. In particular, we will in future simulations increase the size of the computational box in the direction of the magnetic field, to allow sections of larger sunspots to be simulated. The grid separation needs to be reduced in order to adequately resolve the strong vertical gradients associated with radiative cooling in the surface layers and also to represent more accurately the small horizontal scales of the simulated filamentary structures. Reduced grid separation is also needed for a more accurate estimate of the field strengths in the gaps. In the present simulations, the gaps have field strengths on the order of 600–700 G; it is likely that this field strength will be reduced with reduced grid separation. Another desirable improvement concerns the radiative energy transfer; in the present calculations assumed to be grey and represented by a small number of rays only. A binned opacity treatment, and an increased number of rays should be employed in future experiments.

Finally, Doppler and Stokes spectra calculated from the simulation data will allow 'forward modeling' and direct comparisons with dopplergrams and magnetograms.

TH thanks Nordita and DAMTP for financial support and Axel Brandenburg and Wolfgang Dobler for extensive discussions relating to implementation of boundary conditions. ÅN thanks JILA and the Danish Natural Science Research Council (FNU) for support during a sabbatical stay as a JILA Visiting Fellow. Computing time provided by the Danish Center for Scientific Computing (DCSC) is gratefully acknowledged.

REFERENCES

Bray, R. J ., & Loughhead, R. E. 1964, The International Astrophysics Series, London: Chapman Hall, 1964
Carlsson, M., Stein, R. F., Nordlund, Å., & Scharmer, G. B. 2004, ApJ, 610, L137
Hagenaar, H. J., & Shine, R. A. 2005, ApJ, 635, 659
Heinemann, T., 2006, Master's Thesis, Niels Bohr Institute, University of Copenhagen
Heinemann, T., Dobler, W., Nordlund, Å., Brandenburg, A. 2006, A&A, 448, 731
Keller, C. U., Schüssler, M., Vögler, A., & Zakharov, V. 2004, ApJ, 607, L59
Langhans, K., Scharmer, G. B., Kiselman, D., Löfdahl, M. G., & Berger, T. E. 2005, A&A, 436, 1087
Langhans, K., Scharmer, G. B., Kiselman, D., Löfdahl, M. G., 2006, A&A, in press
Leka, K. D., & Skumanich, A. 1998, ApJ, 507, 454
Meyer, F., & Schmidt, H. U. 1968, Mitteilungen der Astronomischen Gesellschaft Hamburg, 25, 194
Nordlund, Å, Stein, R. F. 1990, Proc. IAU Symp. 138 (ed. J. O. Stenflo), Kluwer, 191
Parker, E. N. 1979, ApJ, 234, 333

Rimmele, T., & Marino, J. 2006, ApJ, 646, 593
Rouppe van der Voort, L. H. M., Löfdahl, M. G., Kiselman, D., & Scharmer, G. B. 2004, A&A, 414, 717
Scharmer, G. B., Gudiksen, B. V., Kiselman, D., Löfdahl, M. G., & Rouppe van der Voort, L. H. M. 2002, Nature, 420, 151
Scharmer, G. B., & Spruit, H. C. 2006, A&A, in press
Schlichenmaier, R., Jahn K., Schmidt H. U., 1998a, ApJ, 493, L121
Schlichenmaier, R., Jahn K., Schmidt H. U., 1998b, A&A, 337, 897
Schüssler, M., & Vögler, A. 2006, ApJ, 641, L73
Solanki, S. K., & Montavon, C. A. P. 1993, A&A, 275, 283
Spruit, H. C. 1976, Solar Phys., 50, 269
Spruit, H. C., & Scharmer, G. B. 2006, A&A, 447, 343
Stein, R. F., & Nordlund, A. 1998, ApJ, 499, 914
Steiner, O. 2005, A&A, 430, 691
Sütterlin, P., Bellot Rubio, L. R., Schlichenmaier, R., 2004, A&A, 424, 1049
Thomas, J. H., Weiss, N. O., Tobias, S. M., & Brummell, N. H. 2002, Nature, 420, 390
Tritschler, A., Schlichenmaier, R., Bellot Rubio, L. R., the KAOS Team, Berkefeld, T., & Schelenz. }, T. 2004, A&A, 415, 717
Yang, G., Xu, Y., Wang, H., & Denker, C. 2003, ApJ, 597, 1190